

Document downloaded from:

<http://hdl.handle.net/10251/192208>

This paper must be cited as:

Sarabia Escrivà, E.J.; Soto Francés, VM.; Pinazo Ojer, JM. (2022). Mathematical model based on the radiosity method for estimating the efficiency of in-duct UVGI systems. *Science and Technology for the Built Environment*. 28(9):1255-1269.
<https://doi.org/10.1080/23744731.2022.2079897>



The final publication is available at

<https://doi.org/10.1080/23744731.2022.2079897>

Copyright Taylor & Francis

Additional Information

This is an Author's Accepted Manuscript of an article published in Emilio-José Sarabia-Escriva, Víctor-Manuel Soto-Francés & José-Manuel Pinazo-Ojer (2022) Mathematical model based on the radiosity method for estimating the efficiency of in-duct UVGI systems, *Science and Technology for the Built Environment*, 28:9, 1255-1269, DOI: 10.1080/23744731.2022.2079897

Mathematical model based on the radiosity method for estimating the efficiency of in-duct UVGI systems

Emilio-José Sarabia-Escriba, Víctor-Manuel Soto-Francés, José-Manuel Pinazo-Ojer

Universitat Politècnica de València

Abstract

The article describes a model for calculating the killing ratio of different pathogens with an in-duct ultraviolet (UV) device. The model is based on the radiosity method adapted for the UV radiation range and can be used for analysing any lamp distribution. The paper provides the necessary view factors and the influence of environmental variables (temperature, humidity and air velocity) in the analysis.

The model has been validated using the results of four commercial equipment certificates issued by the US Environmental Protection Agency (EPA). The model results show a high precision on the test results, with a maximum deviation of 9%. In all cases, the model results are lower than that of the test, which allows being on the side of safety in the design.

The model has been programmed in software used by Steril-Air for designing its equipment. Finally, an example of calculating the SARS-CoV-2 killing ratio with a 4x2 lamps arrangement is shown.

Keywords: UVGI; ductwork; air conditioning; in-duct UV

Subject classification codes: include these here if the journal requires them

Introduction

The range of electromagnetic radiation with a wavelength between 200-280 nm is known as ultraviolet waveband C (UVC). This radiation is especially important for its interaction with ribonucleic acid (RNA) and deoxyribonucleic acid (DNA), and thus, for the cellular damage it causes. This effect is used to inactivate microorganisms, therefore air and surfaces disinfection. This germicidal effect is more efficient in the wavelength

range between 260-265 nm (Kowalski 2009). Biasin et al. (Biasin et al. 2021) studied the effects of UVC (254 nm) irradiation on SARS-CoV-2 and pointed out the potential of UVC in inactivating this virus.

The effects of UV on organisms were first described in 1877 by (Downes & Blunt 1877), but it was not until 1937 when the first application appeared. This application consisted of using ultraviolet germicidal irradiation (UVGI) system to control the spread of the measles virus (Wells et al. 1942). Another strategy based on using the UVGI in the ventilation system was described by (Ryan et al. 2011). They observed a significant reduction in cases associated with pneumonia in a neonatal intensive care unit. Nowadays, UVGI systems are used in water, air and surfaces disinfection. UVGI air disinfection has different modes of use: irradiation of the upper-room air (Kanaan et al. 2015); in these cases it is vital to carry out a study to ensure the safety (Hou et al. 2021) and the effectiveness (Noakes et al. 2004) of the system and the quality of the indoor air (Kanaan 2019); irradiation of the entire room when there is no occupancy (Krishnamoorthy & Tande 2016); irradiation of the air through ducts (Luo & Zhong 2021) and irradiation over surfaces. (Reed 2010) extensively analyses the different applications of this technology in air cleaning. Some studies analyse the combination of different disinfection strategies. (Centers for Disease Control and Prevention of U.S. Department of Health and Human Services 2003) recommend using UVGI systems as a complement, not as a substitute, for filters in healthcare facilities.

The health crisis caused by the SARS-CoV-2 virus has highlighted the importance of indoor air quality in buildings. Heating Ventilation and Air Conditioning (HVAC) systems play a fundamental role in the strategy to control the spread of pathogens. Dilution by ventilation, differential pressures in rooms, filtration and UVGI

are the most important strategies for controlling indoor air quality (Francisco et al. 2020).

In-duct UVGI system has two main advantages: first of all, the irradiation occurs outside the occupied area of the rooms; in addition, it can even be done centrally for several rooms. (Levetin et al. 2001) analyse the effectiveness of the UVGI in the air handling units (AHU) of an office building with satisfactory results. Secondly, the interior surfaces of the HVAC system are also disinfected, which reduces maintenance needs (Kowalski 2011). Filters, insulators and cooling coils are ideal environments for the proliferation of different microorganisms (Ahearn et al. 1997). (Ezeonu et al. 1994) related to some infectious diseases and respiratory problems such as rhinitis or asthma (Burge 1990).

Although there are many experimental works related to calculating the efficiency of UVGI systems (Luo & Zhong 2021), the development of models is very poor in this field. Apart from the method described in the article, there are two main methods for estimating the efficiency of UVGI systems: CFD analysis and the ray-tracing method.. (Capetillo et al. 2015) uses computational fluid dynamic (CFD) to model UVGI devices with single, four and eight lamps. They used Fluent to develop the methodology. A model with a cross-section of $0.61 \times 0.61 \text{ m}^2$ and 1.83 m in length was divided into 280,000 cells, defined using the meshing ANSYS module. Each cell had different dimensions depending on the proximity to the lamps. This technique require the use of the discrete ordinates method (Ho 2009) to solve the radiant exchange. (Atci et al. 2020) used the same methodology to evaluate the efficiency of different array configurations with four lamps. For this case it is used hexahedral mesh configurations defined in ANSYS ICEM CFD software. The mesh construction is important in these cases in order to reduce the computational cost. On the other hand, (Lau et al. 2012)

used ray-tracing software to calculate and validate a model using two configurations of lamp arrays. This method has its origin in computer graphics and illumination engineering. The method consists of tracing rays from an emitting source and following the trajectory of each one taking into account reflections, absorptions, etc. The two techniques indicated above manage to obtain accurate results, but require modelling the different configurations in a complex way with scientific software and require high computing power.

A recent report by the (US Department of Energy 2021) shows the need to develop models for the UGVI system design. Having software that allows estimating the efficiency of a UVGI system is essential in this type of industry. The original motivation of this research has been the development of a software for the UV lamp manufacturing company Steril-Air. This paper explains the development of a generic model to calculate the effectiveness of any in-duct UVGI system without the need for high computational power, Figure 1. The model is based on the radiosities method adapted to UVC radiation. It allows estimating the dose received by a particle as it passes through the duct and the killing ratio of any pathogen. The model follows a similar strategy to previous models (Kowalski et al. 2000) but incorporates two fundamental new characteristics: the calculation of diffuse radiation in a more precise way through the radiosity method (Clark & Korybalski 1974) and the possibility of defining a group of lamps arranged in rows and columns. The model has been validated with the experimental data from the certification tests carried out by the US Environmental Protection Agency (EPA) for four commercial equipment.

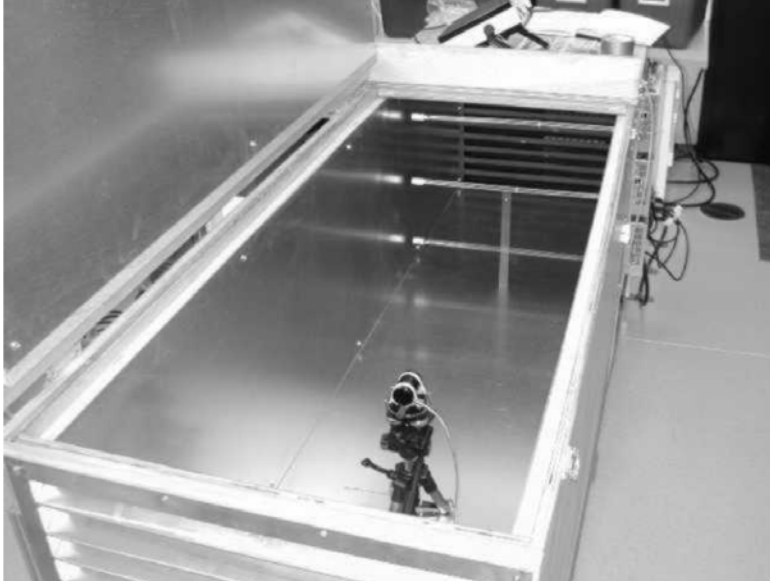


Figure 1. Typical duct section with lamps at the top of the picture. Notice the cooling or heating coil after the lamps. Source (VanOsdell & Foarde 2002).

Methodology

Dose and rate constant for different microorganisms

The surviving ratio of a population for a certain type of microorganism, Sv , is the relation between the number of surviving microorganisms after an amount of time, N_t in contrast to the number of microorganisms at the beginning, N_0 . This value depends on the irradiation received by the microbial, $E_{eff} [\mu W \cdot cm^{-2}]$, the exposure time, $\Delta t [s]$, and the susceptibility of the microorganism, $k [cm^2 \cdot \mu]^{-1}$. The surviving ratio is represented by equation (1) (Kowalski et al. 2000). The product of irradiation and exposure time is known as *Dose* $[\mu J \cdot cm^{-2}]$.

$$\frac{N_t}{N_0} = e^{-kE_{eff}\Delta t} = e^{-kDose} = Sv \quad (1)$$

Therefore, the killing ratio S can be expressed by equation (2).

$$S = 1 - Sv = 1 - e^{-kE_{eff}\Delta t} = 1 - e^{-kDose} \quad (2)$$

Obtaining a value for k for each microorganism is easy when the dose needed for getting a certain killing ratio is known. The Americana air & water (American Air & Water ®) contains many values of the dose for a fixed killing ratio. There are no conclusive data for the case of SARS-CoV-2, but recent studies based on other coronaviruses (Heßling et al. 2020) propose a UV dose of 10,600 $\mu\text{J}\cdot\text{cm}^{-2}$ to get a killing ratio of 90%. As shown in equation (3), the susceptibility constant of each microorganism can be evaluated by clearing this term from equation (2).

$$k = \frac{-\ln(1-S)}{\text{Dose}} = 0,0002172250 \text{ cm}^2 \cdot \mu\text{J}^{-1} \quad (3)$$

Following this procedure for several microorganisms has been obtained Table 1.

Table 1: Dose and empirical constant k for different microorganisms.

Organisms	Dose for a killing ratio	
	of 90% [$\mu\text{J} \cdot \text{cm}^{-2}$]	k [$\text{cm}^2 \cdot \mu\text{J}^{-1}$]
Bacteria		
Bacillus anthracis - Anthrax	4520	0,0005094215
Bacillus anthracis spores - Anthrax spores	24320	0,0000946787
Bacillus magaterium sp. (spores)	2730	0,0008434378
Bacillus magaterium sp. (veg.)	1300	0,0017712193
Bacillus paratyphus	3200	0,0007195578
Bacillus subtilis spores	11600	0,0001984987
Clostridium tetani	13000	0,0001771219
Corynebacterium diphtheriae	3370	0,0006832597
Ebertelia typhosa	2140	0,0010759743
Escherichia coli	3000	0,0007675284
Leptospiracanicola - infectious Jaundice	3150	0,0007309794
Micrococcus candidus	6050	0,0003805926
Micrococcus sphaeroides	1000	0,0023025851

<i>Mycobacterium tuberculosis</i>	6200	0,0003713847
<i>Neisseria catarrhalis</i>	4400	0,0005233148
<i>Phytomonas tumefaciens</i>	4400	0,0005233148
<i>Proteus vulgaris</i>	3000	0,0007675284
<i>Pseudomonas aeruginosa</i>	5500	0,0004186518
<i>Pseudomonas fluorescens</i>	3500	0,0006578815
<i>Salmonella enteritidis</i>	4000	0,0005756463
<i>Salmonella paratyphi</i> - Enteric fever	3200	0,0007195578
<i>Salmonella typhosa</i> - Typhoid fever	2150	0,0010709698
<i>Salmonella typhimurium</i>	8000	0,0002878231
<i>Sarcina lutea</i>	19700	0,0001168825
<i>Serratia marcescens</i>	2420	0,0009514814
<i>Shigella dysenteriae</i> - Dysentery	2200	0,0010466296
<i>Shigella flexneri</i> - Dysentery	1700	0,0013544618
<i>Shigella paradysenteriae</i>	1680	0,0013705864
<i>Spirillum rubrum</i>	4400	0,0005233148
<i>Staphylococcus albus</i>	1840	0,0012514049
<i>Staphylococcus aureus</i>	2600	0,0008856097
<i>Staphylococcus hemolytic</i>	2160	0,0010660116
<i>Staphylococcus lactis</i>	6150	0,0003744041
<i>Streptococcus viridans</i>	2000	0,0011512925
<i>Vibrio comma</i> - Cholera	3375	0,0006822474

Molds

<i>Aspergillus flavus</i>	60000	0,0000383764
<i>Aspergillus glaucus</i>	44000	0,0000523315
<i>Aspergillus niger</i>	132000	0,0000174438
<i>Mucor racemosus</i> A	17000	0,0001354462
<i>Mucor racemosus</i> B	17000	0,0001354462
<i>Oospora lactis</i>	5000	0,0004605170
<i>Penicillium expansum</i>	13000	0,0001771219

Penicillium roqueforti	13000	0,0001771219
Penicillium digitatum	44000	0,0000523315
Rhisopus nigricans	111000	0,0000207440
Protozoa		
Chlorella Vulgaris	13000	0,0001771219
Nematode Eggs	45000	0,0000511686
Paramecium	11000	0,0002093259
Virus		
Bacteriophage - E. Coli	2600	0,0008856097
Infectious Hepatitis	5800	0,0003969974
Influenza	3400	0,0006772309
Poliovirus - Poliomyelitis	3150	0,0007309794
Tobacco mosaic	240000	0,0000095941
	10600 (Heßling et al.	
SARS-CoV-2	2020)	0,0002172250
Yeast		
Brewers yeast	3300	0,0006977531
Common yeast cake	6000	0,0003837642
Saccharomyces cerevisiae	6000	0,0003837642
Saccharomyces ellipsoids	6000	0,0003837642
Saccharomyces spores	8000	0,0002878231

Other models for the killing effect of radiation on microorganisms are also available. For example, two-stage decay model considers that there are two populations with a different k , equation (4). In this case, the surviving ratio uses two different constants, $k_1[\text{cm}^2 \cdot \mu\text{J}^{-1}]$ for the fast decay population and $k_2[\text{cm}^2 \cdot \mu\text{J}^{-1}]$ for the resistant population. The parameter f represents the resistant fraction of the total initial population.

$$Sv = 1 - S = \frac{N_t}{N_0} = (1 - f)e^{-k_1 E_{eff} \Delta t} + f e^{-k_2 E_{eff} \Delta t} \quad (4)$$

However, such precision is not necessary for the described model because this effect is noticeable only in high disinfection ratios (6-log) (Kowalski et al. 2000).

Dose calculation

Figure 2 represents an in-duct UVGI system with a row of lamps positioned perpendicular to the air direction. A straight path inside the duct is also depicted with the entry point at the coordinates XX, ZZ . This path is the shortest that any microorganism can take inside the duct.

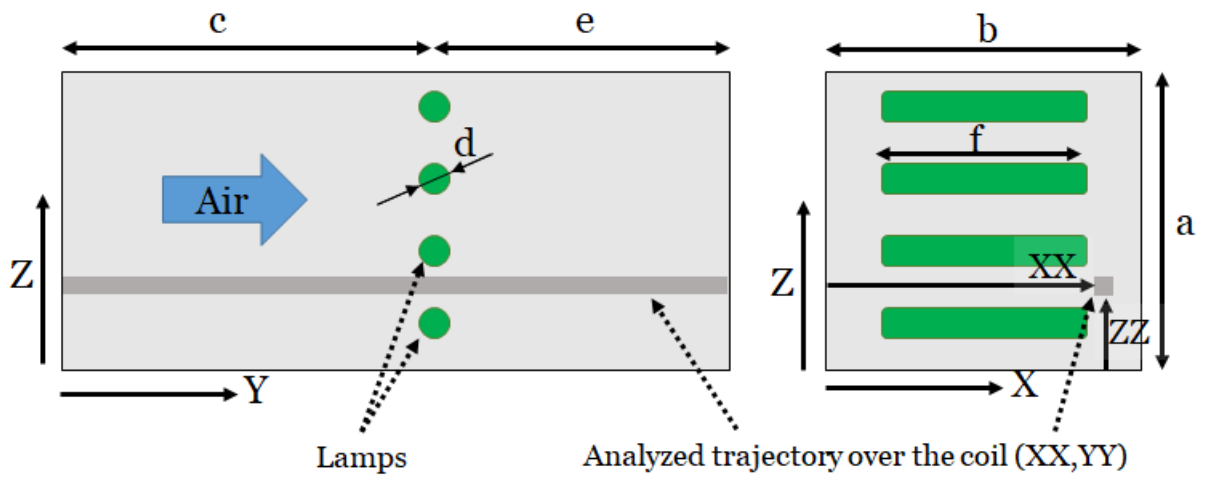


Figure 2. In-duct UVGI system with four lamps in the same row. Side view (left) and front view (right).

To calculate the dose received by the microorganism when passing through the system, the duct is divided into small volumes individually evaluated. For each volume in the position (x,y,z) , the UV intensity $Q(x, y, z)$ [W] is estimated as the sum of direct radiation (from the lamps) and reflected radiation (from the walls).

The mesh used consist of 50 subdivisions for each cross axes (X, Z) and one subdivision for each centimetre in the longitudinal axis (Y). For instance, for a duct 40 cm high, 60 cm wide and 70 cm deep, there are $N_x \cdot N_z \cdot N_y = 50 \cdot 50 \cdot 70$ positions to study.

Assuming a constant radiation intensity inside each subdivision, the dose received in each volume is expressed by equation (5), where $t[s]$ is the exposure time for crossing each subdivision.

$$Dose(x, y, z) = Q(x, y, z) \cdot t \quad (5)$$

The dose received in any straight, $Dose(x, z)$, path is determined by equation (6).

$$Dose(x, z) = \sum_1^{N_y} Dose(x, y, z) \quad (6)$$

The killing ratio obtained for each trajectory, $S(x, z)$, is computed by equation (7).

$$S(x, z) = 1 - e^{k \cdot Dose(x, z)} \quad (7)$$

The average mortality ratio, S_{mean} , is calculated considering all the trajectories, $N_x \cdot N_z = 50 \cdot 50$, equation (8).

$$S_{mean} = \frac{\sum_1^{N_x} \sum_1^{N_z} S(x, z)}{50 \cdot 50} \quad (8)$$

Estimation of the UV radiation at a grid point (x,y,z)

What kills the microorganism is the amount of UVC radiation received. To define the constant k it is necessary to measure the laboratory the energy that arrives at each cm^2 of a population on a plate and to measure how many of them are still alive afterward .

However, when the microorganism is in the air current, the geometry is likely to be close to a sphere, and therefore the radiation arrives from every direction. To be able to compare the data of energy received by an organism considered as a sphere with the data obtained at the laboratory (k values) for a plane, we must consider this latter

surface as a sphere of 4 cm². This relationship appears as a result of the ratio between the surface area of a sphere and that of a circle of the same radio.

The ultraviolet radiation reaching the organism has two components: the radiation coming directly from the lamps and the reflected radiation by the walls. The reflection on the walls can be specular or diffuse. In this work, we have assumed only diffuse reflection. This is justified because although at the beginning, the surface could be very polished and the reflection being specular, it gets dirty quickly. Therefore, the dominant reflection, in practice, is going to be closer to a diffusive mode. This allows using of the radiation view factors to compute the reflection component of the radiation.

The most common materials used inside ducts and their reflective properties in the UV range are shown in Table 2.

Table 2: Reflective properties of the materials.

Material	Reflection coefficient[%]
GalvanisedGalvanised	
Steel	53
Aluminium	74
Aluminium foil	73
Stainless Steel	28
Plastic	10

The radiant properties of the system elements are explained below:

- (1) The lamps, all of them with an outer diameter (O.D.) of 1.5875 cm, emit UV radiation as a function of their length and type (it is commented below).
- (2) The microorganisms only absorb the UV radiation. Therefore, there is neither emission nor reflection.

- (3) Lateral and top walls are diffuse reflecting surfaces whose reflective coefficient depends on the type of material. They are not emitters of UV radiation; they only reflect it partially.
- (4) The cross-sections at the inlet and outlet are usually coils or filters. The first has a large number of fins on the surface, and the latter has a low reflective coefficient. Therefore, it can be considered that they neither emit nor reflect UV radiation.
- (5) There are two possibilities for the bottom wall: The first, they possess the same radiant properties as the lateral walls. The second, there is a pool of water (i.e., the tray of the cooling coil where the condensate is collected). In this case, all the ultraviolet energy is absorbed by the water, and therefore it has the same radiant properties (in the UVC) as the inlet and outlet cross-sections. Obviously, it is not an emitter of UVC.

Once the radiant properties of the surfaces in the UV range have been established, the problem can be solved using any method for calculating radiant energy exchange without participating medium. The radiosities method (Clark & Korybalski 1974) has been chosen for this model because it allows taking into account the multiple reflections easily.

Adaptation of the radiosities method for UV radiation.

The radiosity method was originally developed to calculate the thermal radiant exchange between surfaces of a closed room. Thermal exchange includes the entire wavelength spectrum. However, the model should only consider the interaction in the UVC range. In order to adapt the original radiosity method to the exchange of UV radiation, it is necessary to take into account the following comments:

- In the conventional method, a body (its surface) emits radiation whenever its temperature is higher than 0 K. In contrast, in UV radiation analysis, surfaces do not emit UV radiation (they only reflect it). Therefore, its equivalent temperature for analysis is 0 K.
- The radiant properties of the surfaces are different for each wavelength. The average radiant properties of the surfaces must be considered in the analysis and must correspond to the range of UV radiation.
- Those bodies that absorb UV radiation will have a zero reflection coefficient.

The four surfaces defined in the model and their properties are indicated below, taking into account the previous comments.

- (1) Lamps: their UV radiation power is known, W_{lamp} [W]. It is assumed a reflective coefficient equal to zero for them.
- (2) Microorganism: it absorbs all the UV radiation. Therefore, its reflection coefficient is zero. It does not emit UV radiation; then its equivalent temperature is 0 K.
- (3) Lateral and top walls: the reflective coefficient depends on the material used, Table 2. These surfaces do not emit UV radiation; then they are defined with an equivalent temperature of 0 K.
- (4) Inlet and Outlet cross-section: these surfaces do not reflect UV radiation, so their reflective coefficient is zero. As before, its temperature is assumed to be 0 K.

The bottom wall properties depend on the existence of water or not. If there is water, case 4 above is considered for this surface, and therefore, this surface is included as part of this group of surfaces. Otherwise, if there is no water, the bottom surface

behaves like the lateral and top walls, and then this is integrated into the group described in case 3.

The radiosity method can be defined in a matrix way, equation (9). This matrix relates the radiosity of each surface with the heat flux rates, temperatures, view factors and emissivity of all the system surfaces.

$$\begin{bmatrix} \frac{Q_{lamp}}{A_{lamp}} \\ 0 \\ 0 \\ 0 \end{bmatrix} = \begin{bmatrix} 1 - F_{lamp,lamp} & -F_{lamp,org} & -F_{lamp,w} & -F_{lamp,io} \\ 0 & 1 & 0 & 0 \\ \frac{-(1-\varepsilon)F_{w,lamp}}{\varepsilon} & \frac{-(1-\varepsilon)F_{w,org}}{\varepsilon} & \frac{1-(1-\varepsilon)F_{w,w}}{\varepsilon} & \frac{-(1-\varepsilon)F_{w,io}}{\varepsilon} \\ 0 & 0 & 0 & 1 \end{bmatrix} \begin{bmatrix} W_{lamp} \\ W_{org} \\ W_w \\ W_{io} \end{bmatrix} \quad (9)$$

In this expression, $Q_{lamp}[W]$ is the power in the UV range of the lamp, $A_{lamp} [m^2]$ is the lamp area and $W [W \cdot m^{-2}]$ are the radiosities in the UV. F parameters represent the view factor between surfaces: lamp, organism (org), top and lateral walls (w) and inlet and outlet cross-section surfaces (io). ε is the emissivity of each surface. According to Kirchhoff's law, the emissivity of a surface is equal to the absorption coefficient. In the case of opaque surfaces, this value is calculated as one minus the reflectivity coefficient. Remember that the bottom wall is included either in the io-surfaces (case of a water pool) or in the lateral and top case otherwise (w-surfaces).

Once the radiosities have been obtained, the matrix system is defined to calculate the UV radiation flux rates of each surface (Q), equation (10).

$$\begin{bmatrix} \frac{Q_{lamp}}{A_{lamp}} \\ \frac{Q_{org}}{A_{org}} \\ \frac{Q_w}{A_w} \\ \frac{Q_{io}}{A_{io}} \end{bmatrix} = \begin{bmatrix} 1 - F_{lamp,lamp} & -F_{lamp,org} & -F_{lamp,w} & -F_{lamp,io} \\ -F_{org,lamp} & 1 - F_{org,org} & -F_{org,w} & -F_{org,io} \\ -F_{w,lamp} & -F_{w,org} & 1 - F_{w,w} & -F_{w,io} \\ -F_{io,lamp} & -F_{io,org} & -F_{io,w} & 1 - F_{io,io} \end{bmatrix} \begin{bmatrix} W_{lamp} \\ W_{org} \\ W_w \\ W_{io} \end{bmatrix}$$

(10)

From equation (10), it is possible to obtain the total UV radiation power reaching the microorganism (Q_{org}).

Lamp calibration and ambient factors

The lamps are calibrated by placing a sensor 1 meter away from the lamp and in the middle of its span. The energy arriving at a 1 cm² surface must be measured, Figure 3.

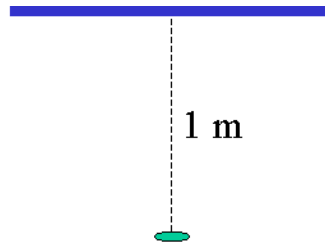


Figure 3. Sketch of the calibration sensor position with respect to the lamp.

The radiation that reaches this small surface can be computed as equation (11).

$$Q_{measured} = Q_{lamp} F_{lamp,element} \quad (11)$$

The view factor $F_{lamp,element}$ can be considered the view factor between a finite surface and a differential one, Figure 4. Therefore, using the reciprocity property of the view factors, equation (12) is obtained.

$$A_{element} F_{element,lamp} = A_{lamp} F_{lamp,element} \quad (12)$$

Assuming that the differential surface is a plane surface of 1 cm², the UV radiation flux rate from the lamp, Q_{lamp} , is calculated with equation (13).

$$Q_{lamp} = Q_{measured} \frac{A_{lamp}}{F_{element,lamp}} \quad (13)$$

The view factor $F_{element,lamp}$ can be considered as the view factor between a differential plane surface with respect to a finite cylinder, Figure 4. This has been calculated by Modest (Modest 2013).

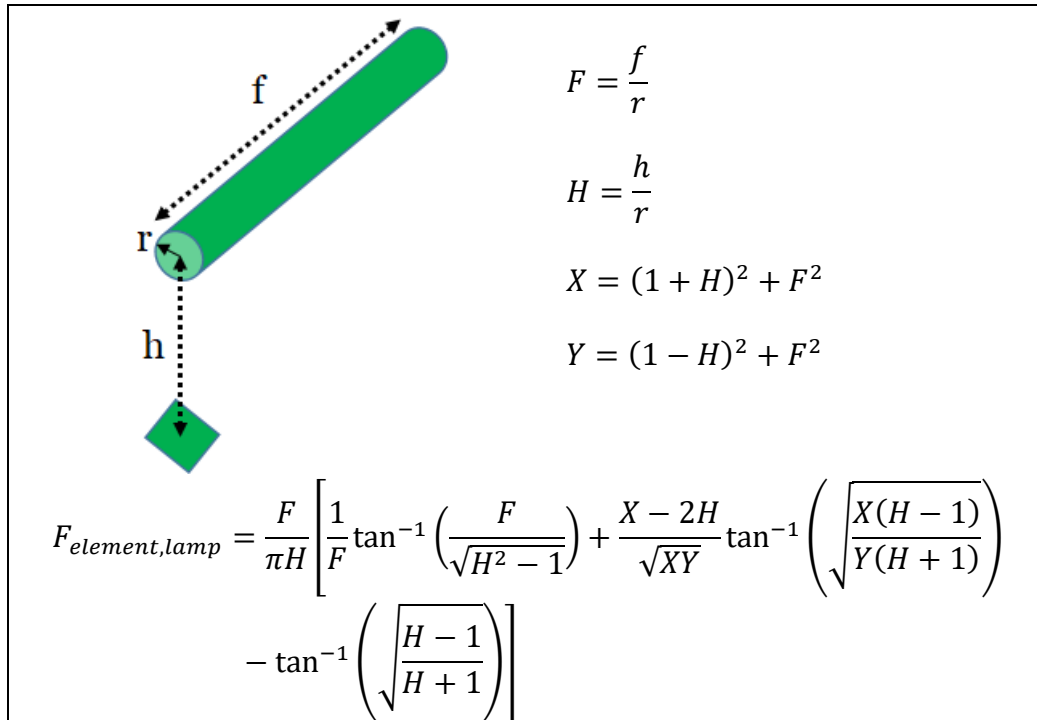


Figure 4. View factor differential element-finite cylinder. The normal passes through one end of a cylinder and is perpendicular to the cylinder axis.

Due to the position of the sensor during the measurement, the total view factor is just the double value of the expression $F_{element,lamp}$ in Figure 4, taking the “f” as one-half of the length of the lamp.

Logically, the amount of UV energy emitted by a lamp depends on the manufacturing process and is practically constant, at least for a manufacturing series. It is shown an example of calibration applied to a series of UV commercial lamps with the following calibration data:

- Arc Length = 34.3 cm
- Diameter = 1.5875 cm
- Distance from the sensor = 100 cm
- Mean power measured = $145 \mu\text{W} \cdot \text{cm}^{-2}$

The intensity obtained with the calibration method is $0.08477 \text{ W}\cdot\text{cm}^{-2}$. Using this value for the commercial lamps GTS16, GTS20, GTS24, GTS30, GTS36, GTS42, we have obtained Table 3, when the length is shown along with the lamp characteristics.

Table 3: Calibration of commercial UV lamps.

Type	Power (UVC) [W]	Electric power [W]	Arc length [cm]	Total length [cm]
GTS16	14.500818	39	34.3	40.64
GTS20	18.428297	51	44.1	50.80
GTS24	23.141788	61	54.2	56.80
GTS30	30.696386	81	69.5	72.19
GTS36	38.865127	98	84.7	87.40
GTS42	47.202377	111	100.0	102.60

There are lamps with an extra rear reflector. This reflector has opposite effects:

- On one hand, no direct radiation from the lamp reaches the microorganism once this has overpassed the lamps. This fact is used when calculating the view factors.
- On the other, this reflector increases a little the amount of UV energy released towards the inlet section of the duct. The mean power measured for a lamp of the same size with reflector is $160 \mu\text{W}\cdot\text{cm}^{-2}$. Therefore, this component increases the power by 10.34%. Table 4 shows the new values for this case.

Table 4: Calibration of commercial UV lamps with rear reflector.

Type	Power (UVC) [W]	Electric power [W]	Arc length [cm]	Total length [cm]
GTS16	16.000902	43	34.3	41.0
GTS22	22.476560	61	50.1	56.8
GTS28	29.919279	81	65.4	72.1

GTS34	36.877490	98	80.7	87.4
GTS40	46.141979	110	95.9	102.6

The amount of UV emitted by a lamp depends on the lamp surface temperature, humidity and air velocity. (Zhang et al. 2020) analyze the effectiveness of UV lamps concerning some environmental parameters. The study observes that the maximum efficiency is found for a temperature range between 20-21°C and decreases with increasing humidity. Using the studies of (VanOsdell & Foarde 2002), it is proposed the following correlations for the correction factor:

- Temperature (T) and air velocity (v) dependency, equation (14).

$$F(T, v) = 2.422333 - 0.0480403T - 0.0002094552T^2 - 1.038712v + 0.126608v^2 + 0.0645444Tv - 0.0001371971T^2v - 0.0105683Tv^2 + 0.00005158034T^2v^2 \quad (14)$$

Range of validity: $0.5 \text{ m} \cdot \text{s}^{-1} < v < 3.4 \text{ m} \cdot \text{s}^{-1}$; $7 \text{ }^\circ\text{C} < T < 28 \text{ }^\circ\text{C}$.

- Humidity dependency (Wh in $\text{kg}_{\text{water}} \cdot \text{kg}_{\text{dry air}}^{-1}$), equation (15).

$$F(Wh) = 1.006 - 1.2001Wh \quad (15)$$

Range of validity: $0.005 \text{ kg}_{\text{water}} \cdot \text{kg}_{\text{dry air}}^{-1} < Wh < 0.02 \text{ kg}_{\text{water}} \cdot \text{kg}_{\text{dry air}}^{-1}$.

The actual power of a lamp under certain conditions can be calculated as equation (16).

$$\frac{Q_{\text{lamp}}}{A_{\text{lamp}}} = \frac{Q_{\text{measured}}}{F_{\text{element, lamp}} \Big|_{\text{calibrated}}} \cdot F(T, v) \cdot F(Wh) \quad (16)$$

In the calibrating conditions $F(T, v)F(Wh) = 1$ and these conditions are $T = 7 \text{ }^\circ\text{C}$, $v = 2 \text{ m} \cdot \text{s}^{-1}$ and $0.005 \text{ kg}_{\text{water}} \cdot \text{kg}_{\text{dry air}}^{-1}$, which correspond with an 80% relative humidity. If the measurement is done in other conditions, the calibrated value in the “standard” conditions could be inferred using the expression above.

It is a known fact that the UV power of a lamp decreases with time (ASHRAE 2008). In our calculation, we let the user introduce a fixed value for this decay factor. Another fact is the maintenance of the lamps. It is not true that the lamps are always clean and assuming the opposite would lead to great errors. Once more, the user should introduce a maintenance factor. A mean value of 80% is recommended.

Necessary view factors

The computation of the view factors is usually a tedious or complex matter, but many books have compiled a series of view factors (Howell et al. 2010). These view factors should be used together with the view factors' properties: such as the addition and the reciprocity.

For the view factor between a small sphere and a finite cylinder, it has been substituted the cylinder by a plane with the same length and width. This plane is perpendicular to a line passing through the centre of the sphere and lying on the cylinder axis.

The lamps are finite cylinders and therefore, their interfering effect must be considered in the view factors among all the surfaces. For instance, such is the case for the exchange between the inlet and outlet surfaces or the reduction in the reflected amount of energy towards the microorganism due to the presence of the lamps.

Finally, it must be noticed that it is necessary to compute how many lamps are seen by the microorganism in each position. For example, when the position analysed is closed to the column of lamps, the microorganism only "sees" the two nearest lamps (one above and one below) but not all the lamps. In this case, the direct radiation only comes from these two lamps.

Figure 5, Figure 6, Figure 7, Figure 8 and Figure 9 show the reference view factors necessary to calculate the view factors between the four surfaces of the model.

- Finite cylinder with respect to a plane of differential area (integrating this over the differential element, a finite-finite view factor can be obtained)

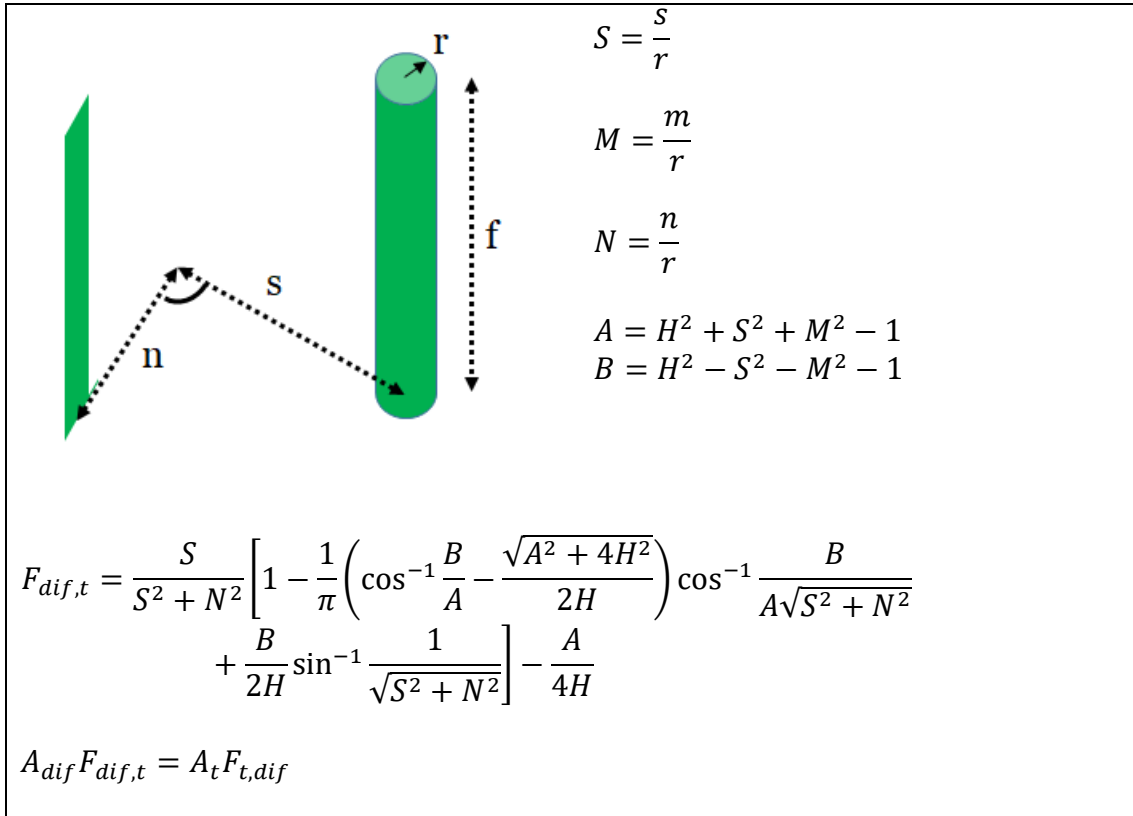


Figure 5: Finite cylinder with respect to a plane of differential area.

- Finite cylinder with respect to the finite cylinder. (Parallel axis. Figure 6)

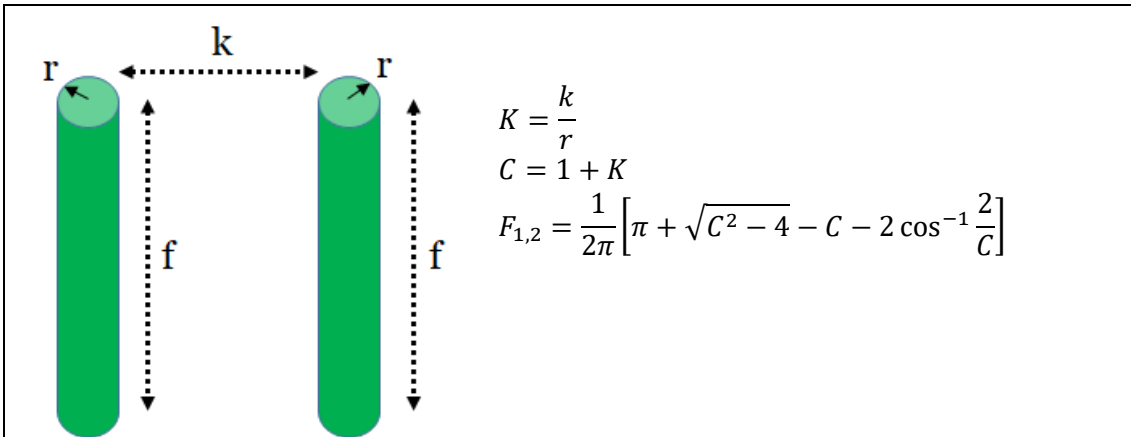


Figure 6: Finite cylinder with respect to the finite cylinder

- Sphere with respect to a plane of finite area:

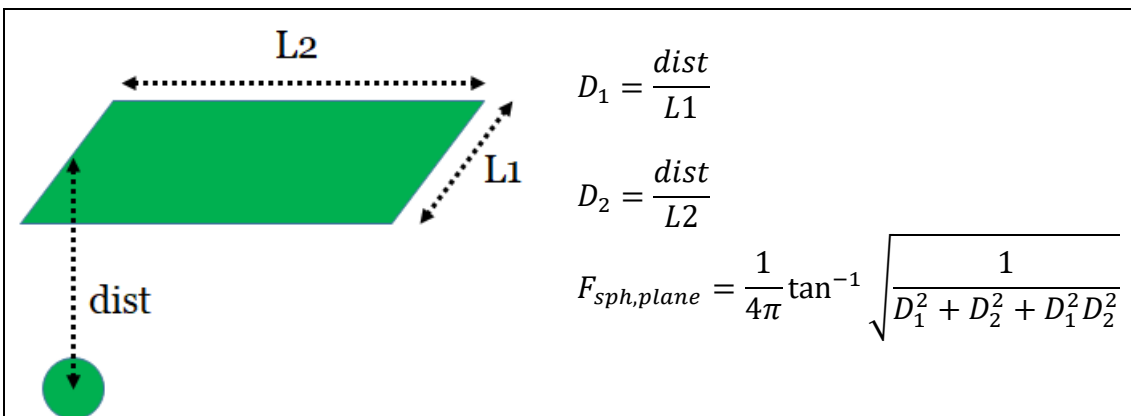
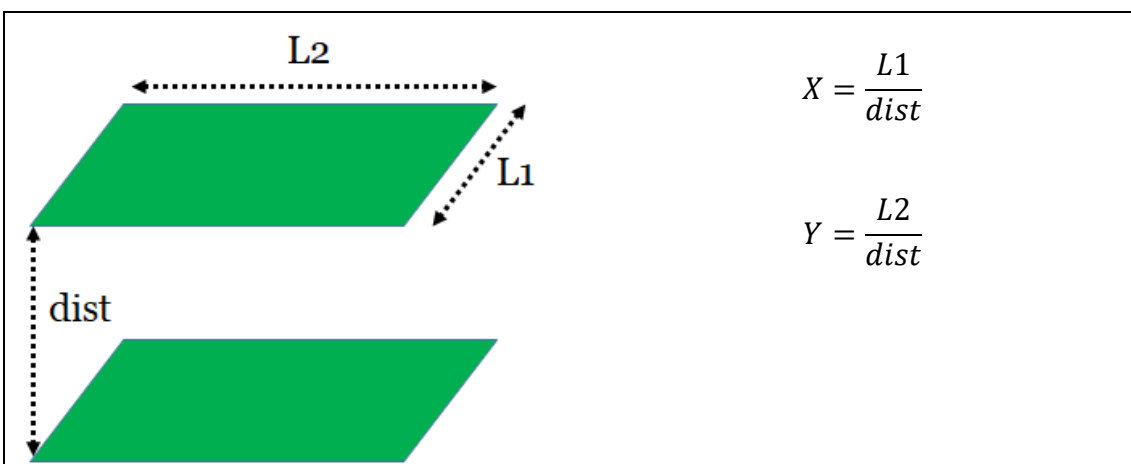


Figure 7: Sphere with respect to a plane of finite area

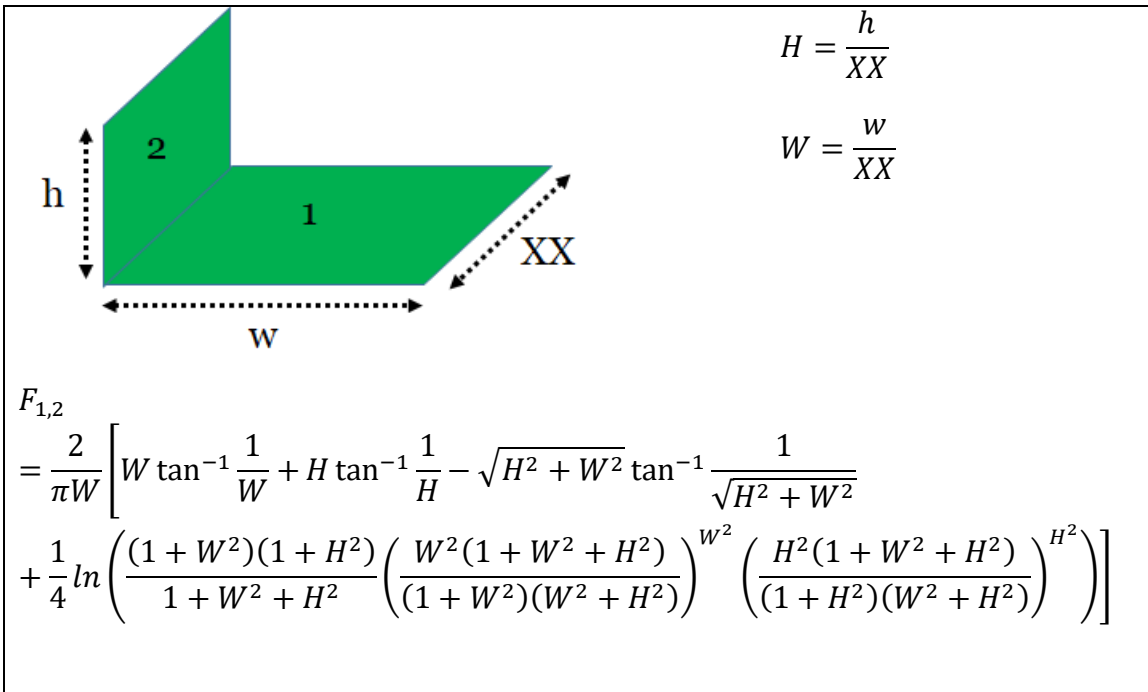
- Finite plane with respect to a parallel finite plane:



$$F_{1,2} = \frac{2}{\pi XY} \left[\ln \left(\frac{(1+X^2)(1+Y^2)}{1+X^2+Y^2} \right)^{0.5} + X\sqrt{1+Y^2} \tan^{-1} \frac{X}{\sqrt{1+Y^2}} + Y\sqrt{1+X^2} \tan^{-1} \frac{Y}{\sqrt{1+X^2}} - X \tan^{-1} X - Y \tan^{-1} Y \right]$$

Figure 8: Finite plane with respect to a parallel finite plane

- Finite plane with respect to a finite perpendicular plane



$$H = \frac{h}{XX}$$

$$W = \frac{w}{XX}$$

$$F_{1,2} = \frac{2}{\pi W} \left[W \tan^{-1} \frac{1}{W} + H \tan^{-1} \frac{1}{H} - \sqrt{H^2 + W^2} \tan^{-1} \frac{1}{\sqrt{H^2 + W^2}} + \frac{1}{4} \ln \left(\frac{(1+W^2)(1+H^2)}{1+W^2+H^2} \left(\frac{W^2(1+W^2+H^2)}{(1+W^2)(W^2+H^2)} \right)^{W^2} \left(\frac{H^2(1+W^2+H^2)}{(1+H^2)(W^2+H^2)} \right)^{H^2} \right) \right]$$

Figure 9: Finite plane with respect to a finite perpendicular plane.

Model validation

Firstly, the model has been validated with bibliography data. The result of the proposed model has been compared with the values measured by (Kowalski et al. 2000). Table 5 summarizes the test parameters. The pathogen used was *Bacillus subtilis*, its constant rate is $0.000449 [cm^2 \cdot \mu J^{-1}]$.

Table 5. Test parameters are defined in (Kowalski et al. 2000).

Number of lamps	1
Type	TUV36 PL-L
Power UV-C	24 W
Height of the duct	30 cm
Width of the duct	64 cm
Length of the duct	91 cm
Air Temperature	22 °C
Relative humidity	45%
Volumetric flow rate	0.9439 m ³ ·s ⁻¹
Velocity	4.877 m·s ⁻¹
Reflection coefficient	57.4 %
Floor-type	Reflecting floor

The model developed by Kowalski et al. (Kowalski et al. 2000) shows a predicted killing rate range between 27.5%-28.2 %, while the measured killing rate is 31%. The ratio killing obtained using the new model described in this paper is 30.2%, which shows a better approximation to the measured value.

The following data used for the verification of the model correspond to the US Environmental Protection Agency (EPA) results in the certification of UV commercial equipment. The test method used by this agency for in-duct UV equipment is described in (VanOsdell & Foarde 2002). According to this agency, commercial equipment undergoes this test to determine their effectiveness. One of the pathogens used in this test is the virus bacteriophage MS2 ($k=0.000448 [cm^2 \cdot \mu J^{-1}]$) and its inactivation efficiency (killing ratio) has been taken for validating the developed model. Table 6 summarizes the parameters for different commercial systems and configurations evaluated by EPA. There are no precise specifications regarding the reflection

coefficient of the equipment used in the test. As it is aluminium sheet ducts, a reflectivity coefficient of 75% is taken.

Table 6. A summary of EPA test parameters for in-duct UV devices and model results.

	600/R-06/050	600/R-06/054	600/R-06/055	DC24-6-120
EPA report	(EPA 2006a)	(EPA 2006b)	(EPA 2006c)	(Corporation)
Number of lamps	1	4	4	6
Total UV	19 W	81 W	34 W	132 W
Arc length	53.3 cm	53.3 cm	53.3 cm	53.3 cm
Lamp diameter	1.9 cm	1.9 cm	1.9 cm	1.9 cm
Height of the duct	61 cm	61 cm	61 cm	61 cm
Width of the duct	61 cm	61 cm	61 cm	61 cm
Length of the duct	183 cm	183 cm	183 cm	183 cm
Temperature [°C]	22.8 °C	23.0 °C	23.0 °C	23.1°C
Relative humidity	45%	45%	45%	45%
Volumetric flow rate	3349 m ³ ·h ⁻¹	3349 m ³ ·h ⁻¹	3349 m ³ ·h ⁻¹	3349 m ³ ·h ⁻¹
Velocity	2.5 m·s ⁻¹	2.5 m·s ⁻¹	2.5 m·s ⁻¹	2.5 m·s ⁻¹
Reflection coefficient	74%	74%	74%	74%
MS2 killing ratio (test)	39%	75%	46%	99%
MS2 killing ratio (model)	30%	73%	45%	91%

The last two rows of the Table 6 show the results obtained with the biological test and the model. The model shows a high precision in the 4-lamps devices, while the equipment with one lamp and the equipment with six lamps present a higher ratio than the one calculated by the model. In the case of the equipment with six lamps, the report indicates that the power of the lamps is approximate, and observing the terminology

used for the equipment; we can guess that the power of the lamps may be 24W each, which would increase the calculated ratio at 92.3%.

The model shows a trend of results slightly lower than the actual data; this may be because the model always calculates a straight path through the duct, which implies the minimum time of radiation exposure. In contrast, real paths are more turbulent and it means longer exposure times and therefore, higher killing ratios.

Example of dose calculation and killing index

In this section, it is presented an example of calculating the killing index for a UVGI system. Table 7 shows the characteristics of the UVGI system used as an example.

Table 7. Input data for a particular problem.

Lamps

Number of lamps	8
Number of columns	2
Numbers of rows	4
Type	GTS16
Power UV-C	14.501 W
Arc length	34.3 cm
Lamp diameter	1.587 cm
Reduction due to maintenance	100 %
Reduction due to life cycle	100 %

Duct and Lamps arrangement

Height of the duct	50 cm
--------------------	-------

Distance of the 1° lamp to the floor (a in Figure 12)	6.30 cm
Distance between lamps (height) (d in Figure 12)	12.50 cm
Width of the duct	100 cm
Distance from the lamp to the walls (f in Figure 12)	7.90 cm
Distance between lamps (wide) (g in Figure 12)	15.70 cm
Length of the duct	80 cm
Distance of the surface of the coil from the lamps	30 cm

Air conditions

Temperature	7 °C
Relative humidity	80%
Volumetric flow rate	3600 m ³ ·h ⁻¹
Velocity	2 m·s ⁻¹

Reflective properties of the walls

Reflection coefficient	50 %
Floor-type	Reflecting floor

Figure 10 shows a schematic of the UVGI system to be designed. This example consists of two columns of lamps with three rows each. In this case, all the lamps will be the same, type GTS16, marketed by (steril-aire).

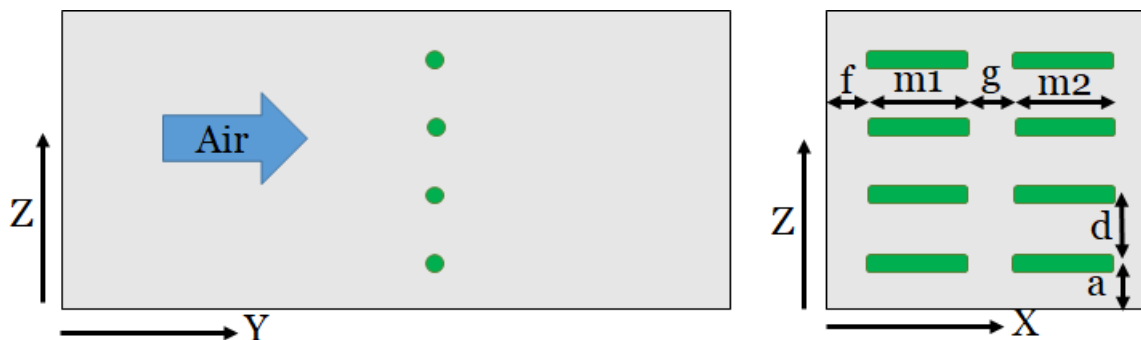


Figure 10. Front and lateral view of the arrangement of the lamps.

Figure 11 shows the total, direct or beam, and diffuse radiation that reaches the microorganism that crosses the duct following a straight line at $x=20$ cm, $z=10$ cm. The total dose received by the microorganism during the path is $7860 \mu\text{J}\cdot\text{cm}^{-2}$, $4978 \mu\text{J}\cdot\text{cm}^{-2}$ direct from the lamps and $2882 \mu\text{J}\cdot\text{cm}^{-2}$ due to reflections.

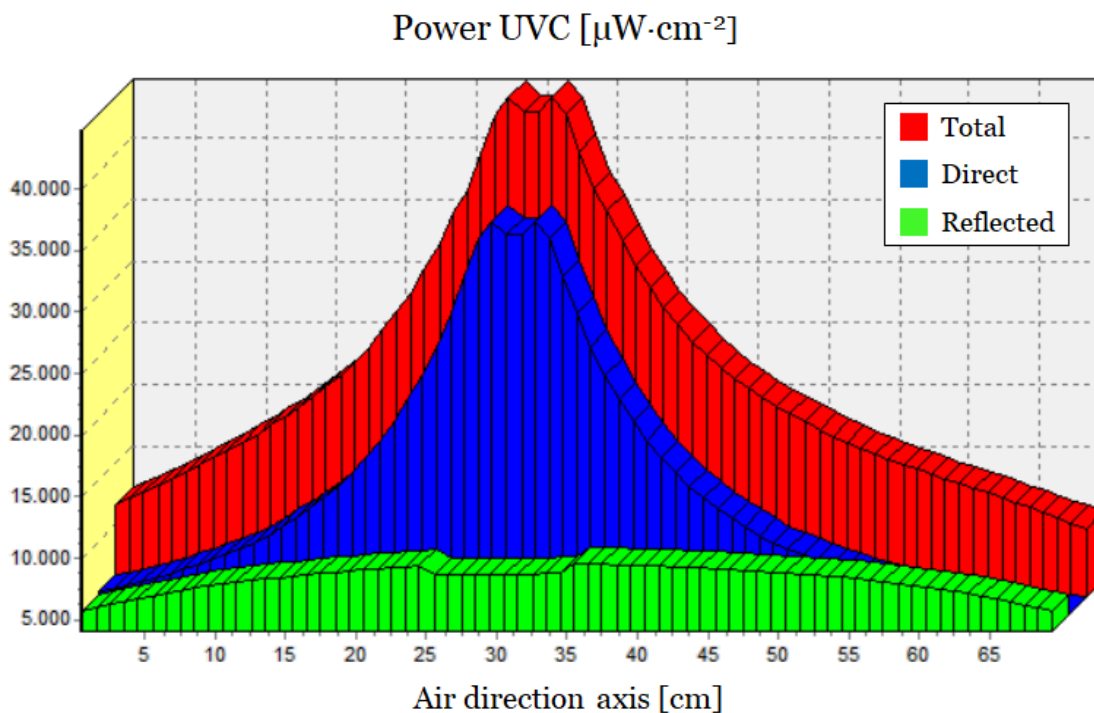


Figure 11. Power in the UV-C range that reaches the microorganism along the line path of coordinates $x=20$ cm, $z=10$ cm.

Remarks:

- The reflected component is relatively less than the beam component. They are of the same order, only far away from the lamps.
- A small valley is observed around $y=30$ cm because the organism sees a lesser amount of lamps (only two, one above and one below).

The same computation for a line passing through $x=20$ cm $z= 20$ cm, in this case, goes very close to one lamp (Figure 12). In this case, the total dose received by the microorganism along the path is $9056 \mu\text{J}\cdot\text{cm}^{-2}$, $6303 \mu\text{J}\cdot\text{cm}^{-2}$ direct and $2753 \mu\text{J}\cdot\text{cm}^{-2}$ by reflexions.

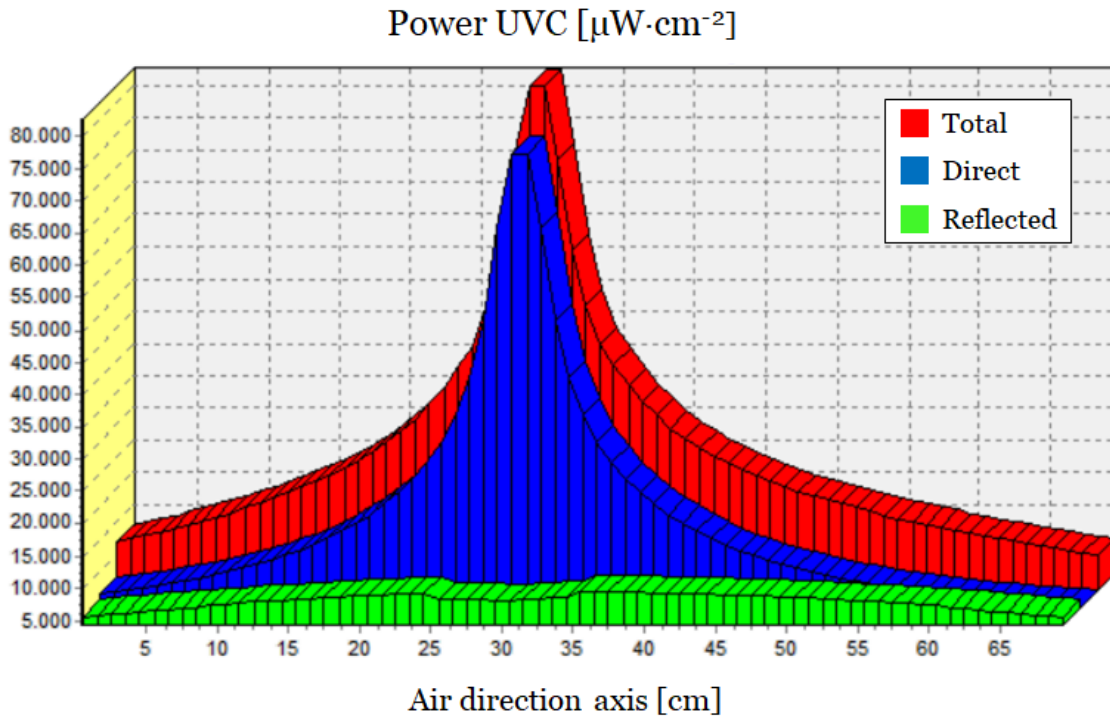


Figure 12. Power in the UV-C range that reaches the microorganism along the line path of coordinates $x=20$ cm, $z=20$ cm.

We observe that the beam radiation has a considerable variation. The reflected component is almost independent of the position along the duct and generally independent of the position inside the duct. Therefore, as the total radiation changes with the line chosen to cross the duct, the killing index must also function as the line chosen. We have made a map for the killing ratio index of the SARS-CoV-2 virus as a function of the line selected along the duct, Figure 13.

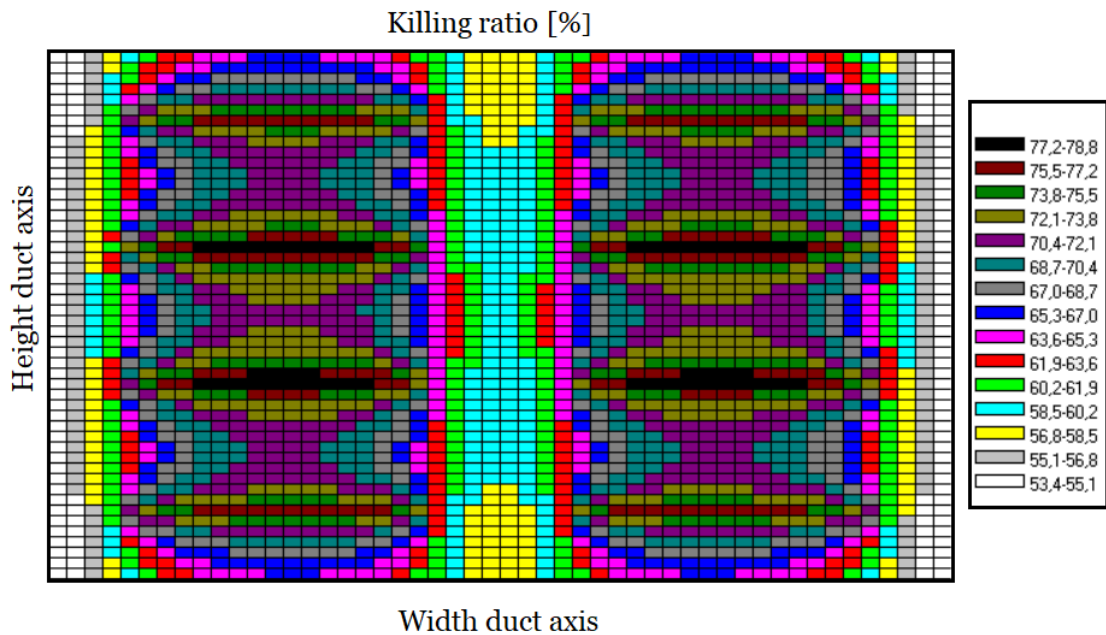


Figure 13. Killing ratio map for the lamp arrangement example and the SARS-CoV-2.

The mean killing ratio obtained for SARS-CoV-2 is 67.3%. The map, Figure 15, shows clearly where the lamps are located; the lines going very near the lamps are the ones with the highest killing index. This value drops to 58.1% if a water pool is used on the floor. On the other hand, the ratio could increase up to 76.7% using the following lamps in the series, the GTS20 model. The calculated values correspond to a straight path along the duct, the minimum path that the microorganism will have. This result, therefore, is conservative and allows us to be on the side of caution in the design of the UGVI device.

Conclusions

In this work, a known method of energy radiation calculation (Clark & Korybalski 1974) has been extended to obtain the dose and the killing ratio of microorganisms when germicide UV lamps are used in an air duct. The method is based on the subdivision of the air duct into small volumes: the transverse area is divided into 250 subdivisions (50 for each axis), while the length of the duct has one subdivision per cm.

This division allows an analysis of the radiation dose received by the microorganism along a minimal path within the duct. If the path is not straight, the dose received will be higher, and therefore the design remains on the conservative side.

Some modifications improve the model with respect to the existing models: the diffuse radiation calculation uses the radiosity methodology, which allows to calculate the indirect radiation accurately on the microorganism; and the model allows for defining a group of lamps arranged in rows and columns, taking into account the obstruction effects that they produce with respect to each other in the microorganism path through the duct. As in other methods, microorganisms have been modelled as a sphere, since this is a geometry more general than previous approaches (cube 1 cm³). Therefore the view factor is closer to reality.

The model has been validated with the data obtained in the tests carried out by the EPA to certify the biological inactivation efficiency of commercial equipment. It has been used the result of six devices with different lamp arrangements. In three of them, the model presents a deviation of less than 2% in calculating the killing ratio. In the other three, the maximum deviation is 9%. In all cases, the model has results below the test; it allows to design of equipment with a margin of safety. Then this methodology can be considered for the design and evaluation of in-duct UVGI systems.

The current limitation of the model implemented in the software developed for Steril-Air is that all lamps must be defined in the same plane and perpendicular to the air direction. In subsequent studies, the analysis of lamps in different planes and positions will be carried out. The radiosity methodology on which the model is based will remain the same, but for these new arrangements, it will be necessary to calculate new view factors between lamps and surfaces.

References

Ahearn DG, Crow SA, Simmons RB, Price DL, Mishra SK, Pierson DL. 1997. Fungal colonization of air filters and insulation in a multi-story office building: production of volatile organics. *Curr Microbiol.* 35(5):305–308.

American Air & Water ® I. www.americanairandwater.com [Internet]. [accessed 2021 Apr 10]. <https://www.americanairandwater.com/>

ASHRAE. 2008. Ultraviolet lamp systems. In: *Ashrae Handb - Syst Equip* [Internet]. [place unknown]. https://www.ashrae.org/file_library/technical_resources/covid-19/si_s16_ch17.pdf

Atci F, Cetin YE, Avci M, Aydin O. 2020. Evaluation of in-duct UV-C lamp array on air disinfection: A numerical analysis. *Sci Technol Built Environ.* 27(1):98–108.

Biasin M, Bianco A, Pareschi G, Cavalleri A, Cavatorta C, Fenizia C, Galli P, Lessio L, Lualdi M, Tombetti E, et al. 2021. UV-C irradiation is highly effective in inactivating SARS-CoV-2 replication. *Sci Rep.* 11(1):6260.

Burge H. 1990. Bioaerosols: prevalence and health effects in the indoor environment. *J Allergy Clin Immunol.* 86(5):687–701.

Capetillo A, Noakes CJ, Sleigh PA, Capetillo A, Noakes CJ, Sleigh PA. 2015. Computational fluid dynamics analysis to assess performance variability of in-duct UV-C systems Computational fluid dynamics analysis to assess performance variability of in-duct UV-C systems. *Sci Technol Built Environ.* 4731.

Centers for Disease Control and Prevention of U.S. Department of Health and Human Services. 2003. Healthcare Infection Control Practices Advisory Committee (HICPAC):

Guidelines for Environmental Infection Control in Health-Care Facilities. US Dep Heal Hum Serv Centers Dis Control Prev Atlanta, GA 30329 [Internet].(July):1–235.

http://www.cdc.gov/hicpac/pdf/guidelines/eic_in_hcf_03.pdf

Clark JA, Korybalski ME. 1974. Algebraic methods for the calculation of radiation exchange in an enclosure. *Wärme- und Stoffübertragung*. 7(1):31–44.

Corporation AU. Environmental Technology Verification Biological Inactivation Efficiency by HVAC In-Duct Ultraviolet Light Systems American Ultraviolet Corporation.

Downes A, Blunt TP. 1877. The Influence of Light upon the Development of Bacteria. *Nature* [Internet]. 16(402):218. <https://doi.org/10.1038/016218a0>

EPA. 2006a. Technology evaluation report Biological Inactivation Efficiency by HVAC In-Duct Ultraviolet Light Systems Biological Inactivation Efficiency by HVAC In-Duct Ultraviolet Light Systems Dust Free Bio-Fighter 4Xtreme, Model 21. Epa 600/R-06/050.

EPA. 2006b. Biological inactivation efficiency by HVAC in-duct ultraviolet light. American Ultraviolet Corporation. ACP-24/HO-4. Epa 600/R-06/054.

EPA. 2006c. Technology evaluation report Biological Inactivation Efficiency by HVAC In-Duct Ultraviolet Light Systems Biological Inactivation Efficiency by HVAC In-Duct Ultraviolet Light Systems Atlantic Ultraviolet Corporation AeroLogic Model AD24-4. Epa 600/R-06/055.

Ezeonu IM, Noble JA, Simmons RB, Price DL, Crow SA, Ahearn DG. 1994. Effect of relative humidity on fungal colonization of fiberglass insulation. *Appl Environ*

Microbiol. 60(6):2149–2151.

Francisco PW, Emmerich SJ, Schoen LJ, Hodgson MJ, Mccoy WF, Miller SL, Li Y, Kong H, Olmsted RN, Sekhar C, et al. 2020. ASHRAE Position Document on Airborne Infectious Diseases by ASHRAE Board of Directors. Ashrae Stand [Internet].:26 pp. www.ashrae.org

Heßling M, Hönes K, Vatter P, Lingenfelder C. 2020. Ultraviolet irradiation doses for coronavirus inactivation - review and analysis of coronavirus photoinactivation studies. GMS Hyg Infect Control. 15:Doc08.

Ho CK. 2009. Radiation Dose Modeling in FLUENT ® Modeling Approach. In: NM: Sandia National Laboratories, editor. WEF Disinfect 2009 Work Model UV Disinfect using CFD [Internet]. University of North Carolina. Albuquerque. https://www.sandia.gov/cfd-water/files/Fluent_DO_presentation.pdf

Hou M, Pantelic J, Aviv D. 2021. Spatial analysis of the impact of UVGI technology in occupied rooms using ray-tracing simulation. Indoor Air. 31(5):1625–1638.

Howell JR, Menguc MP, Siegel R. 2010. Thermal Radiation Heat Transfer, 5th Edition [Internet]. [place unknown]: CRC Press. <https://books.google.es/books?id=FBjSBQAAQBAJ>

Kanaan M. 2019. CFD optimization of return air ratio and use of upper room UVGI in combined HVAC and heat recovery system. Case Stud Therm Eng. 15.

Kanaan M, Ghaddar N, Ghali K, Araj G. 2015. Upper room UVGI effectiveness with dispersed pathogens at different droplet sizes in spaces conditioned by chilled ceiling and mixed displacement ventilation system. Build Environ [Internet]. 87:117–128.

<http://dx.doi.org/10.1016/j.buildenv.2015.01.029>

Kowalski W. 2009. Ultraviolet Germicidal Irradiation Handbook. 1st ed. [place unknown]: Springer, Berlin, Heidelberg.

Kowalski W. 2011. UVGI for Cooling Coil Disinfection, Air Treatment, and Hospital Infection Control. [place unknown].

<http://scholar.google.com/scholar?hl=en&btnG=Search&q=intitle:UVGI+for+Cooling+Coil+Disinfection+,+Air+Treatment+,+and+Hospital+Infection+Control#2>

Kowalski WJ, Bahnfleth WP, Witham DL, Severin BF, Whittam TS. 2000.

Mathematical modeling of ultraviolet germicidal irradiation for air disinfection. *Quant Microbiol.* 2(3):249–270.

Krishnamoorthy G, Tande BM. 2016. Improving the effectiveness of ultraviolet germicidal irradiation through reflective wall coatings: Experimental and modeling based assessments. *Indoor Built Environ [Internet].* 25(2):314–328.

<https://doi.org/10.1177/1420326X14547785>

Lau J, Bahnfleth W, Mistrick R, Kompore D. 2012. Ultraviolet irradiance measurement and modeling for evaluating the effectiveness of in-duct ultraviolet germicidal irradiation devices. *HVAC\&R Res [Internet].* 18(4):626–642.

<https://www.tandfonline.com/doi/abs/10.1080/10789669.2011.611575>

Levetin E, Shaughnessy R, Rogers CA, Scheir R. 2001. Effectiveness of germicidal UV radiation for reducing fungal contamination within air-handling units. *Appl Environ Microbiol.* 67(8):3712–3715.

Luo H, Zhong L. 2021. Ultraviolet germicidal irradiation (UVGI) for in-duct airborne

bioaerosol disinfection : Review and analysis of design factors. *Build Environ* [Internet]. 197(December 2020):107852.

<https://doi.org/10.1016/j.buildenv.2021.107852>

Modest MF. 2013. *Radiative Heat Transfer* [Internet]. Third Edit. Modest MF, editor. Boston: Academic Press.

<https://www.sciencedirect.com/science/article/pii/B9780123869449500017>

Noakes CJ, Beggs CB, Sleigh PA. 2004. Modelling the Performance of Upper Room Ultraviolet Germicidal Irradiation Devices in Ventilated Rooms: Comparison of Analytical and CFD Methods. *Indoor Built Environ* [Internet]. 13(6):477–488.

<https://doi.org/10.1177/1420326X04049343>

Reed NG. 2010. The history of ultraviolet germicidal irradiation for air disinfection. *Public Health Rep.* 125(1):15–27.

Ryan RM, Wilding GE, Wynn RJ, Welliver RC, Holm BA, Leach CL. 2011. Effect of enhanced ultraviolet germicidal irradiation in the heating ventilation and air conditioning system on ventilator-associated pneumonia in a neonatal intensive care unit. *J Perinatol.* 31(9):607–614.

steril-aire. [accessed 2021 Apr 16]. <https://www.steril-aire.com/>

US Department of Energy. 2021. *Lighting R&D Program: Germicidal Ultraviolet (GUV) R&D Meeting.* (February).

VanOsdell D, Foarde K. 2002. *Defining the Effectiveness of UV Lamps Installed in Circulating Air Ductwork.* [place unknown].

Wells WF, Wells MW, Wilder TS. 1942. *THE ENVIRONMENTAL CONTROL OF*

EPIDEMIC CONTAGION: I. AN EPIDEMIOLOGIC STUDY OF RADIANT
DISINFECTION OF AIR IN DAY SCHOOLS. *Am J Epidemiol* [Internet]. 35(1):97–
121. <https://doi.org/10.1093/oxfordjournals.aje.a118789>

Zhang H, Jin X, Nunayon SS, Lai ACK. 2020. Disinfection by in-duct ultraviolet lamps
under different environmental conditions in turbulent airflows. *Indoor Air*. 30(3):500–
511.